

# Acoustic Travel-Time Tomography: Optimal Positioning of Transceiver and Maximal Sound-Ray Coverage of the Room

Najmeh Sadat Dokhanchi, Jörg Arnold, Albert Vogel and Conrad Völker  
*Bauhaus-University Weimar, 99423 Weimar, Germany, email: najmeh.sadat.dokhanchi@uni-weimar.de*

## Introduction

The technique of Acoustic travel-time TOMography (ATOM) can be applied to determine certain properties namely the temperature and flow velocity in a propagation medium [1, 3, 6]. The reason is the dependency between the temperature  $T$  and also flow velocity  $v$  and the speed of sound  $c$  within the medium [1, 3, 4, 5]. Therefore,  $T$  and  $v$  can be determined by measuring the travel time of an acoustic signal from a sound transmitter (loud speaker) to a receiver (microphone) at defined propagation paths. Then, the detected speed of sound can be converted into spatially distributed temperature or flow velocity of the medium using a tomographic reconstruction algorithm [1, 3].

In order to test the application of the ATOM technique for indoor climate measurements, investigations were carried out in a special climate chamber lab of the Bauhaus-University Weimar. For this purpose, impulse responses of the climatic chamber were measured and compared with simulation results of an image source model (ISM). A challenging task is distinguishing the reflections of interest in the reflectogram when the sound-rays have similar travel-times. This paper presents a novel numerical method to address this problem by finding optimal positions of transmitter and receiver since they have a direct impact on the distribution of travel times. These optimal positions have the minimum number of simultaneous arrival times within a threshold level where the threshold level results from differences between the lengths of the sound paths and the resolution of the measuring equipment.

Moreover, for the tomographic reconstruction, when some of the voxels (volumetric grid cells) remain empty of sound-rays, it leads to inaccurate determination of the air temperature within those voxels. The reason is that the temperature can be estimated only from averaging over neighbouring voxels. Based on the presented numerical method, this shortcoming has been addressed by minimizing the number of empty tomographic voxels to ensure the best sound-ray coverage of the room. Subsequently, a spatial air temperature distribution is estimated by simultaneous iterative reconstruction technique (SIRT). The experimental set-up in the climate chamber verifies the simulation results.

## Theoretical background

This principle that the speed of sound in a medium is a function of the medium temperature is the basis of acoustic travel time measurement. In dry air, the speed of sound  $c$  shows a first-order dependence on

temperature under adiabatic conditions can be written as [3]

$$c = \sqrt{\gamma \cdot R_s \cdot T_{av}}, \quad (1)$$

where  $\gamma = 1.4$  is the ratio of the specific heats at constant pressure and volume of the gas,  $R_s = 287.05 \text{ Jkg}^{-1}\text{K}^{-1}$  is the specific gas constant for dry air, and  $T_{av}$  is a ‘virtual temperature’ of the gas, taking into account the specific humidity and is defined as

$$T_{av} = (1 + 0.513q)T, \quad (2)$$

where  $q$  is specific humidity which is the ratio of water vapor mass to the total mass of moist air and  $T$  is the temperature of the gas in  $K$ .

To calculate the speed of sound, the travel-time of an acoustic signal is measured along known sound paths. For this purpose, the impulse response is determined by cross-correlation technique between transmitted and received signals. Therefore, an MLS signal (maximum length sequences) is used as an excitation signal [3] with the sequence length of  $2n - 1$ , where  $n$  is the number of digital shift registers.

The temperature along known propagation paths is determined by the travel-time estimation of an acoustic signal. The measured travel-time of an acoustic signal  $\tau$  along a sound path  $l$  within a room can be calculated by [3],

$$\tau = \int_l \frac{l}{c(r)} dl = \int_l s(r) dl. \quad (3)$$

where  $c(r)$  is the spatially variable speed of sound,  $s(r)$  is the slowness which is a reciprocal value of the speed of sound and  $r$  is the position inside the tomographic area. To extract the delay-time between the emitted and the received signal, cross-correlating technique is used [3]. The result of the cross-correlation is the impulse response of the room (IR) including the arrival time of the direct sound as well as the reflections. The locations of the maxima in the cross-correlation function indicate the temporal lag between the transmitted and received signals, representing the travel-time of the signal [5]. In order to highlight the low order reflections, kurtosis method is applied to the reflectogram after cross-correlation calculation [3].

In the ISM method, the travel-times of the sound-rays along different paths are calculated based on the geometry of the room and the known positions of transmitter and receiver, using the geometric law of reflection. The mathematical approach applied in this work to derive the impulse response of the room using ISM method is described in [3] in full detail.

For tomographic reconstruction of the temperature distribution, SIRT is employed to convert the detected speeds of sound into spatially distributed temperatures. The calculation process of the slowness distribution of given tomographic voxels applying SIRT method are given by [1].

## Numerical method

### Optimal Positioning of Transmitter and Receiver:

When the sound source transmits an acoustic signal to the measurement environment, the signal will be propagated through the space, hits the boundary surfaces and resulting in several reflections. Subsequently, the direct sound and afterwards reflections will be received by microphone at a certain time. Since one of the main tasks of the ATOM technique is to detect these travel-times, the sound paths are required to be separated properly. Therefore, in order to have distinguishable travel-times in the reflectogram, the position of the sound-source and receiver should be determined to have the minimum number of simultaneous arrival times. This problem is addressed by presenting a numerical method in which the optimal coordinates of transmitter and receiver are achieved for the examined rectangular room.

To specify possible coordinates for positioning of the sound-source and receiver, each dimension of the room is divided into certain parts. Consequently, these spatial coordinates provide the total number of feasible locations for placement of the sound-source and receiver. Hence, the optimal position of transmitter and receiver can be calculated using the following equation

$$S = \min_{k \in \{1, \dots, K\}} M_k, \quad (4)$$

$$M_k = \sum_{i=1}^n \sum_{j=i+1}^n \mathbb{I}(|L_i^{(k)} - L_j^{(k)}| \leq \Delta),$$

where  $n$  is the total number of sound paths,  $L_i^{(k)}$  and  $L_j^{(k)}$  are the lengths of the sound paths corresponding to the  $i$ -th and the  $j$ -th reflected path,  $K$  is the number of spatial coordinates corresponding to different locations of transmitter and receiver,  $\Delta$  is a threshold level chosen appropriately according to the differences between the lengths of the sound paths and the resolution of the measuring equipment, i.e.  $|L_i^{(k)} - L_j^{(k)}|$ .  $\mathbb{I}$  is the indicator function of equation (4) given in the following form

$$\mathbb{I}(x) := \begin{cases} 0 & \text{if } x \text{ is false;} \\ 1 & \text{if } x \text{ is true.} \end{cases} \quad (5)$$

where  $\mathbb{I}(x)$  maps elements of  $x$  to the range of 0, 1. It takes into account the cases in which the value of the  $|L_i^{(k)} - L_j^{(k)}|$  is less than  $\Delta$ . As a result, equation (4) considers the solutions by finding the minima of the sum of the number of cases that their differences between the length of the paths are less than a desired threshold level. These optimal coordinates of the sound source and receiver allow separation of the travel-times in the recorded reflectogram.

### Maximal Sound-Ray Coverage of the Room:

In the tomographic reconstruction, the sound-rays should travel through all parts of the room. If some of the voxels are remained empty of sound-rays, it degrades the accuracy of the temperature measurement within those voxels. For this purpose, an additional function is employed in the numerical method to calculate the number of empty tomographic voxels as follows

$$\mathcal{A} = \min_{s \in \{1, \dots, |S|\}} N_s, \quad (6)$$

$$N_s = \sum_{v=1}^{\xi} \mathbb{I}(l_v^{(s)} = 0)$$

where  $\xi$  is total number of voxels and  $l_v^{(s)}$  is sum of the lengths of sound-rays in meter existing in the  $v$ -th voxel corresponding to the  $s$ -th member of  $S$  (see equation (4)). The best sound-ray coverage of the room is determined by calculation of the minimum of the number of empty tomographic voxels. Therefore, by adding this method to the optimal solutions of (4), the optimal positions of the transmitter and receiver in terms of maximal sound-ray coverage of the room can be obtained.

### Example of optimization

Based on the numerical method presented in the previous section, the optimal position of a sound-source and a receiver is calculated for a 3 m × 3 m × 2.44 m climate chamber lab of the Bauhaus-University Weimar. More details about the characteristic of the climate chamber are provided in [8]. Each dimension of the room is divided into 20 segments, therefore, the total number of feasible coordinates is  $K = 20^3$ . The threshold level is set to  $\Delta = 0.5 \text{ ms} \times c$  ( $c = 343.4 \text{ m/s}$  as an initial value at  $T = 20^\circ\text{C}$ ) determined based on the path length differences. To simulate the theoretical sound-ray paths up to second order reflections, the same convention of the ISM used in [1, 3] has been applied. Table 1 shows the positions of the sound-source and receiver for both an optimal and a non-optimal case.

**Table 1:** Calculated positions

Alternatives	Coordinates	
	source	receiver
1. Opt-position (calculated)	$x = 0.69 \text{ m}$	$x = 0.25 \text{ m}$
	$y = 1.72 \text{ m}$	$y = 0.69 \text{ m}$
	$z = 1.18 \text{ m}$	$z = 0.60 \text{ m}$
2. Non-opt-position (randomly selected)	source	receiver
	$x = 1.72 \text{ m}$	$x = 2.24 \text{ m}$
	$y = 1.72 \text{ m}$	$y = 0.25 \text{ m}$
	$z = 1.18 \text{ m}$	$z = 0.60 \text{ m}$

The optimal position is calculated based on the numerical method, however, the non-optimal position is chosen randomly. In order to clarify the differences between various positions of the source and receiver, the optimal case is compared with the non-optimal case (see Figure 1). Figure 1a shows the non-optimal case in which there

are several sound-rays arrived simultaneously. Figure 1b illustrates that there are no sound paths with simultaneous sound-rays arrival time up to second order reflections. It demonstrates the optimal position of the sound-source and receiver leads to an optimized distribution of travel times in the reflectogram.

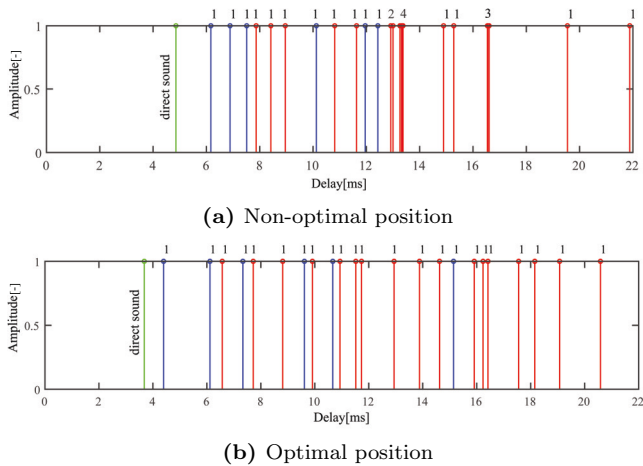


**Figure 1:** Comparing the reflectograms of (a) non-optimal and (b) optimal case. The green line is the direct sound path arrival time. The blue and red lines are the first and second order reflections, respectively. The order means how many times a sound signal is reflected at the room boundaries when traveling along the sound path from transmitter to receiver [3]. The number above the lines shows the number of sound paths arriving at that certain time within the threshold level of 0.1 ms.

It is required to solve the both optimization problems of (4) and (6), while equation (4) avoids sound-rays overlap on the reflectogram and equation (6) gives the maximum sound-ray coverage. There is a trade-off between the results of equation (4) and (6). When there is a symmetry in the relative location of sound-source and receiver, maximum sound-ray coverage can be achieved but this leads to many overlapping sound-rays. On the other hand, when there is no symmetry, it generates non-overlapping sound rays but the coverage becomes poor.

## Experimental set-up

The measurement was carried out in the climate chamber lab of the Bauhaus-University Weimar [8]. Figure 2 shows the measurement set-up including the location of the transmitter, receiver and NTC thermistors. For the tomographic reconstruction, the volume of the room has been divided into  $3^3 = 27$  voxels. Therefore, the volume of each voxel is  $(x \cdot y \cdot z) = (1\text{m} \cdot 1\text{m} \cdot 0.81\text{m})$ . In the first experiment, a sound-source and a receiver were located at the calculated optimal position (see Table 1).

To verify the ‘tomographically reconstructed temperature’ values, fifteen negative temperature coefficient thermistors (NTC) with an accuracy of  $\pm 0.1\text{K}$  were applied at the center of each of fifteen (randomly chosen) tomographic voxels. These fifteen NTC thermistors enable a more precise comparison of temperatures within the voxels. The distance in height and width between each

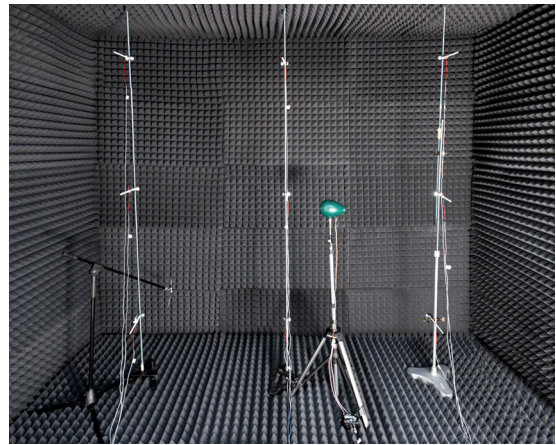


**Figure 2:** Experimental set-up in the climate chamber lab of the Bauhaus-University Weimar. The absorbing panels have been applied to the climate chamber in order to uniquely identify reflections in the reflectogram.

sensor are  $0.81\text{m}$  and  $1\text{m}$  respectively. A measurement interval of 10 seconds is selected based on the length of the excitation signal and the power of the computer for execution of cross-correlation, kurtosis analysis and tomographic reconstruction [3].

The second experiment has been done for one non-optimal position (see Table 1) with the same condition and the results of the temperature distribution of the two cases were compared together. For both experiments, the climate chamber has been configured to be at steady state condition and the measurements have been carried out at a uniform air temperature of  $20\text{ }^\circ\text{C}$ . As the climate chamber is tempered by the surfaces, an air velocity can be excluded.

For the measurements, a standard 1/4-inch condenser microphone of type ‘AVM8 MI-17’ and for the sound-source, a special self-constructed speaker (with the 2-inch broadband driver FRS 5 XTS by VISATON) was used. The sound-source is developed to have a nearly omni directional point source specification detailed in [2]. For data acquisition, the measurement card ‘Data Translation DT9847-2-2’ is used which is a dual channel dynamic signal analyser with two analogue outputs and two analogue inputs. The digitization rate of 216 kHz leading to a good resolution for processing of signals which is required for the small dimensions of the climate chamber lab. For the sampling frequency of 216 kHz, the excitation time of the MLS signal is 1.21s. The software package used to analyse the data is MATLAB R2017b.

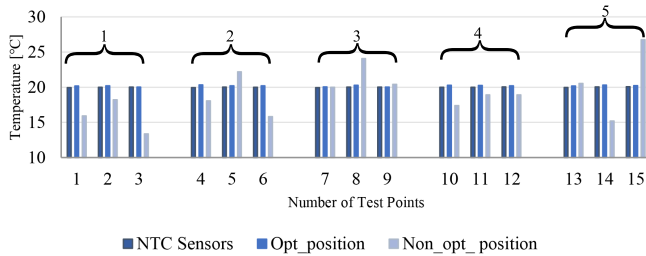
## Travel-time correction

Various factors (e.g. is described in [7]), such as the uncertainty of the geometrical positioning of the sound-source and receiver, synchronization errors of the transmitted and recorded signals, and inaccuracy of a physical hardware may produce deviation in the travel-time measurement of the signal. Therefore, the offset values of the travel-times caused by these uncertainties must be determined. For this purpose, all reflections up to second order have been measured and detected individually

by applying absorbing panels to the boundary surfaces of the climate chamber. The absorbing panels helped to have a clearer reflectogram for detecting the reflection of interest. For this experiment, the climate chamber has been arranged again to be in steady state condition at a uniform air temperature of 20 °C. Consequently, the determined offset values have been considered in the simulation model.

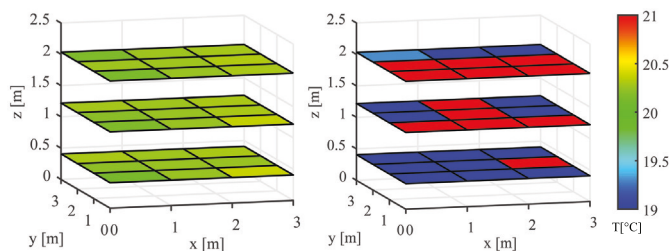
## Measurement results and data analysis

Figure 3 shows the mean tomographically reconstructed temperatures (ATOM-temperatures) of the 15 randomly chosen tomographic voxels for both the optimal and the non-optimal position in five clusters, each composed of three temperature layers (three superimposed voxels). It compares the temperatures of the NTC thermistors at the corresponding locations with ATOM-temperatures. In the optimal case, the mean ATOM-temperatures within determined voxels are in a good agreement with the temperatures of NTC thermistors. However, in the non-optimal case, the influence of simultaneous arrival time of the sound-rays can be observed as a great deviation of temperature between ATOM and NTC thermistors. The overlapping of the reflections in the reflectogram of the non-optimal case obviously affects the results of the air temperature.



**Figure 3:** Comparison of the temperatures of the NTC thermistors at the corresponding locations with ATOM-temperatures. For the optimal position, there is a good agreement between the ATOM and NTC temperatures.

Figure 4 shows the tomographically reconstructed distributions of ATOM-temperatures for the optimal position (Left) and the non-optimal position (Right). The temperature distribution of the optimal case has a good match with the real temperature in contrast to the non-optimal case.



**Figure 4:** Tomographically reconstructed temperature distribution determined with ATOM technique; (Left) optimal position, (Right) non-optimal position.

## Conclusions

In this study, a numerical calculation presented to determine an optimal position of sound-source and receiver within a measurement environment. In order to measure the spatially distributed indoor air temperature by ATOM as accurately as possible, a high resolution of reflectogram is required. It means the arrival time of the sound-rays should be distinguishable. In addition, this approach was able to achieve a good sound-ray coverage of the room as well.

## Acknowledgments

The authors would like to show their gratitude to the Thüringer Graduiertenförderung. Additionally, we highly appreciate the scientific collaboration with the institute of meteorology, University of Leipzig. Their support is highly cherished and appreciated.

## References

- [1] BARTH, M. ; RAABE, A.: Acoustic tomographic imaging of temperature and flow fields in air. In: *Measurement Science and Technology* 22 (2011), Nr. 3, S. 035102
- [2] BLEISTEINER, M.: *Ableitung von Raumtemperaturverteilungen aus Schallreflexionsmessungen*. Technische Universität Berlin, 2014
- [3] BLEISTEINER, M. ; BARTH, M. ; RAABE, A.: Tomographic reconstruction of indoor spatial temperature distributions using room impulse responses. In: *Measurement Science and Technology* 27 (2016), Nr. 3, S. 035306
- [4] BOHN, D. A.: Environmental effects on the speed of sound. In: *Audio Engineering Society Convention 83* Audio Engineering Society (Veranst.), 1987
- [5] HOLSTEIN, P. ; RAABE, A. ; MÜLLER, R. ; BARTH, M. ; MACKENZIE, D. ; STARKE, E.: Acoustic tomography on the basis of travel-time measurement. In: *Measurement Science and Technology* 15 (2004), Nr. 7, S. 1420
- [6] JOVANOVIĆ, I. ; SBAIZ, L. ; VETTERLI, M.: Acoustic tomography method for measuring temperature and wind velocity. In: *2006 IEEE International Conference on Acoustics Speech and Signal Processing Proceedings* Bd. 4 IEEE (Veranst.), 2006, S. IV–IV
- [7] VECHERIN, S. N. ; OSTASHEV, V. E. ; WILSON, D. K.: Assessment of systematic measurement errors for acoustic travel-time tomography of the atmosphere. In: *The Journal of the Acoustical Society of America* 134 (2013), Nr. 3, S. 1802–1813
- [8] VÖLKER, C. ; MÄMPEL, S. ; KORNADT, O.: Measuring the human body's microclimate using a thermal manikin. In: *Indoor air* 24 (2014), Nr. 6, S. 567–579